

Modular Construction and Deconstruction of Organic Solar Cells

Jeffrey M. Mativetsky and Yueh-Lin Loo

Dept. of Chemical and Biological Engineering, Princeton University, Princeton, NJ 08544

DOI 10.1002/aic.13923

Published online September 28, 2012 in Wiley Online Library (wileyonlinelibrary.com).

Keywords: organic solar cells, organic semiconductors, solution processing, soft-contact lamination

Introduction

At 1,000 W/m², the sun delivers an enormous amount of energy to the Earth's surface. If we can harness this energy without losses, an hour's worth of sunlight will be sufficient to power all human activities for a year. It is for this reason that solar cells—devices that directly convert sunlight to electricity—have received tremendous attention. Current solar cell technologies based on inorganic semiconductors, however, remain too costly for widespread deployment. An alternative that is gaining increasing research attention is organic solar cells, that is, solar cells built with electrically active organic small molecules and polymers. Large-scale chemical synthesis of these materials and low-temperature, scalable processing, such as inkjet or roll-to-roll printing, offer new paradigms for device production and the potential to reduce both capital and manufacturing costs.^{1–3} Organic materials are also chemically customizable, lightweight, and flexible, opening up new opportunities for building- and vehicle-integrated applications.

Through the development of new organic semiconductors,^{4,5} improved film processing,^{6,7} and refined device architectures,^{8,9} record performance organic solar cells have breached the 10% efficiency milestone,¹⁰ widely considered the threshold for commercial viability.^{2,11} Improved understanding of the links between molecular structure, materials processing, film morphology, and device performance promises to yield further gains. Chemical engineers are equipped to address issues to deliver functionally efficient and cost-effective solar cells in an integrated and systematic manner.

Why Modular?

Although organic electronics offer new approaches to device fabrication, device assembly still—like conventional semiconductor electronics—relies on a sequence of irreversible processing steps involving the deposition and patterning of thin layers of semiconductors, conducting interconnects, and dielectrics. Imagine instead electrical contacts or semiconducting active layers that can be reversibly and nondestructively inserted and removed, electrically connected and disconnected. The development of soft-contact lamination (ScL) has brought to bear such versatility at the laboratory scale, opening up a modular approach to organic device fabrication and characterization.

Modular device construction yields both technological and fundamental benefits. In multilayered device architectures, ScL allows for the independent optimization of individual layers before assembly into devices. Moreover, after the device is built and tested, the now-buried layers can be exposed and systematically characterized, replaced, or modified. Finally, new device architectures that are otherwise inaccessible can be constructed.

Noninvasive electrical contact to organic thin-film transistors^{12–14} and light-emitting diodes^{15,16} has previously been achieved through ScL, resulting in significantly reduced contact resistances and fewer pinhole defects in the respective devices. ScL has also been employed to integrate and test novel electrode materials in organic solar cells.^{17,18} In this Perspective article, we will highlight recent progress on the use of ScL to characterize organic solar cells in ways previously not possible.

Organic Semiconductors

Organic semiconducting molecules possess sp²-hybridized, conjugated backbones, resulting in delocalized π orbitals. For charges to traverse from molecule to molecule, overlap between π orbitals of adjacent molecules is necessary. Molecular packing—i.e., the degree of intermolecular order and the relative orientation of molecules with respect to one

Correspondence concerning this article should be addressed to Y.-L. Loo at lloo@princeton.edu.

Current address of J. M. Mativetsky: Dept. of Physics, Applied Physics and Astronomy, Binghamton University, Binghamton, NY 13902.

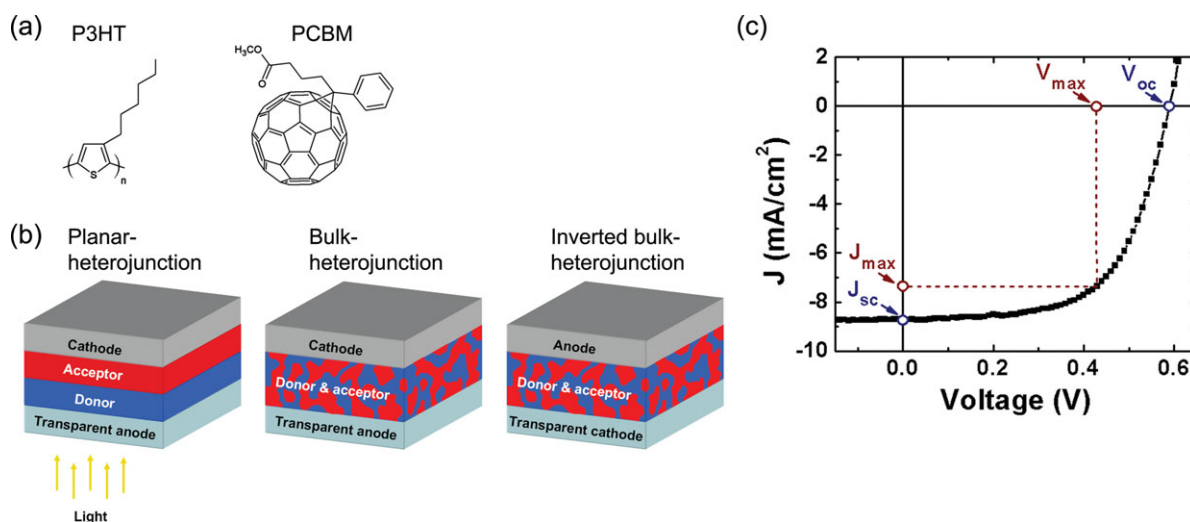


Figure 1. (a) Chemical structures of commonly employed electron donor (P3HT), and electron acceptor (PCBM), (b) Schematic of planar-heterojunction (left) and bulk-heterojunction (middle) solar cells constructed in the conventional configuration, and a bulk-heterojunction (right) solar cell constructed in the inverted configuration.

Light enters the solar cells through the transparent electrodes at the bottom. Buffer layers, often included at the electron- and hole-collecting interfaces, are not shown for simplicity, and (c) J-V characteristics of a P3HT:PCBM bulk-heterojunction solar cell constructed in the conventional configuration; the J-V characteristics of an inverted solar cell would appear in the second quadrant exhibiting a positive J_{sc} and a negative V_{oc} .

another—thus figures prominently in dictating the charge transport properties of organic semiconductors. Highly crystalline organic semiconductor films, for example, have yielded thin-film transistors with charge carrier mobilities beyond 1 cm²/Vs, exceeding that of amorphous silicon. Devices comprising amorphous organic semiconductors, on the other hand, have often exhibited mobilities that are several orders of magnitude lower. Given that the details of processing can dramatically influence molecular packing in organic semiconductor thin films, the ability to tune processing conditions is often a means by which the optoelectronic properties of such films can be manipulated.

In the active layers of organic solar cells, two organic semiconductors are needed, one serving as an electron donor and the other as an electron acceptor. The transfer of photo-excited electrons from the electron donor to the electron acceptor takes place by virtue of an energy offset between the two. More specifically, the lowest-occupied molecular orbital (LUMO) of the electron donor is higher in energy, i.e., closer to the vacuum level, than that of the electron acceptor, allowing electron transfer from the LUMO of the electron donor to the LUMO of the electron acceptor when photogenerated excitons dissociate at the donor-acceptor interface. A further requisite for solar cell operation is that the donor effectively transports holes, while the acceptor transports electrons. In principle, organic semiconductors are intrinsically capable of transporting both types of charge carriers; such ambipolar transport, however, is more the exception than the rule. Extrinsic effects, such as interfacial charge trapping and oxidation, tend to trap electrons making electron transport less common than hole transport.^{19,20} In the context of organic solar cells, poly(3-hexyl-thiophene), P3HT, and [6,6]-phenyl C₆₁ butyric acid methyl ester, PCBM, whose chemical structures are shown in Figure 1a, are the most commonly stud-

ied electron donor and acceptor pair. However, new organic semiconductors are constantly being developed, yielding rapid and continual improvements in organic solar cells performance over the last decade.^{4,5,21,22}

Organic Solar Cell Architectures

The simplest organic solar cell geometry is the bilayer, or planar-heterojunction architecture, in which a pristine interface is formed between the electron donor and the electron acceptor (see Figure 1b). When light passes through the transparent anode, normally indium tin oxide (ITO), it is absorbed by the electron donor. This process generates excitons, i.e., Coulombically bound electron-hole pairs, which then diffuse within the electron donor layer. The exciton diffusion length, limited by its lifetime, ranges from several nanometers up to tens of nanometers.^{23,24} If the exciton reaches the donor-acceptor interface at which there is sufficient energetic driving force for dissociation, it separates into free charge carriers. The electron is then transferred to and transports through the electron acceptor, eventually making its way to the cathode. The hole remains in and transports through the electron donor to the anode for photocurrent collection. Buffer layers are sometimes inserted at the electron- and hole-collecting interfaces to limit reactivity between the electrode and active layer molecules, metal penetration during deposition, or the transport of minority charge carriers.²⁵ A low-work function metal, such as aluminum, is used as the cathode to collect electrons.

A major limitation of the planar heterojunction architecture is that the active layer thickness cannot simultaneously satisfy the conditions required for optimal light absorption and exciton dissociation. Given typical extinction coefficients

of electron donors, the light-absorbing layer must have a thickness on the order of 100–200 nm to effectively absorb incoming sunlight. On the other hand, light-generated excitons can only diffuse about one tenth of that distance before they relax to the ground state. A thick light-harvesting layer will thus absorb a large fraction of incoming light, but the majority of the generated excitons will decay to the ground state before they can dissociate into free charges. Alternatively, a thin active layer will convert all its light-generated excitons into free charges, but such a device will be limited by the amount of light that it absorbs.

This conundrum is addressed by an alternative architecture, called the bulk-heterojunction (BHJ),⁸ also shown in Figure 1b. In the BHJ architecture, the active layer consists of interpenetrating nanoscale domains of electron donor and acceptor. The mixed layer is thick enough to absorb most incoming light. At the same time, a high density of donor-acceptor interfaces provides for efficient exciton dissociation. For these reasons, BHJ solar cells exhibit higher photocurrent outputs and efficiencies compared to planar-heterojunction devices, despite challenges in controlling and characterizing the complex nanoscale morphology within the active layers.^{6,7,26}

The output current density-voltage (J-V) characteristics of a representative P3HT:PCBM BHJ solar cell are shown in Figure 1c. The efficiency (*eff*) is defined as the ratio of the maximum power density generated P_{\max} —i.e., the point at which the product of current density J , and voltage V , is maximum (J_{\max} and V_{\max} , respectively)—and the incident light power density P_{in} :

$$\text{eff} = \frac{P_{\max}}{P_{\text{in}}} = \frac{J_{\max} V_{\max}}{P_{\text{in}}}$$

There are several important metrics used to describe solar cell performance. For the purposes of this article, other than efficiency, we will focus on three main performance indicators: the current density when no voltage is applied is referred to as the short-circuit current density J_{sc} ; the voltage when no current passes is the open-circuit voltage V_{oc} ; and the fill factor *FF*, is defined as

$$FF = \frac{J_{\max} V_{\max}}{J_{\text{sc}} V_{\text{oc}}}$$

These parameters are individually labeled in Figure 1c for clarity. The J_{sc} depends on the efficiencies of all of the processes responsible for current generation, i.e., light absorption, exciton diffusion, exciton dissociation, charge transport, and charge collection. The V_{oc} generally correlates with the energy level difference between the highest-occupied molecular orbital (HOMO) of the electron donor and the LUMO of the electron acceptor.^{4,27,28} The difference in the work functions of the electrodes can also play a role.^{18,29} Finally, the *FF* is the ratio of the maximum power density generated to the maximum theoretical power density based on the J_{sc} and V_{oc} . The fill factor is highly sensitive to parasitic series and parallel resistances within the device.

Another important consideration in building organic solar cells is their air stability. Molecular design and encapsulation strategies are under development to minimize detrimental environmental effects on the organic components.³⁰

Degradation of the low-work function electrode is another concern, as commonly employed metals in use as cathodes oxidize readily. To address this latter issue, solar cells are often constructed in the inverted configuration.^{31,32} In inverted solar cells, the transparent electrode is used as a cathode to collect electrons rather than as an anode to collect holes (Figure 1b). A titania layer at the electron-collecting interface serves to block the transport of holes to ITO while a high-work function metal, such as gold, is used as top contact to collect holes, allowing the device to operate under ambient conditions. Given the opposite placements of the anode and cathode with respect to conventional solar cells, the J-V characteristics of inverted devices appear in the second quadrant with positive J_{sc} and negative V_{oc} , as opposed to in the fourth quadrant with negative J_{sc} and positive V_{oc} .

Organic Solar Cell Fabrication

Organic solar cells are multilayered devices, normally constructed in a sequential, layer-by-layer fashion. Transparent bottom electrodes, usually ITO supported on glass, are photolithographically defined. Subsequent buffer and active layers are often cast from solution, although vacuum deposition is sometimes employed with materials exhibiting limited solubility in organic solvents. Solution processing at the laboratory scale is typically achieved by spin-coating, while scalable methods, such as doctor blading, spray-coating, and printing are actively explored as well.^{2,3} BHJ active layers are prepared by casting a cosolution comprising the electron donor and acceptor, and then using subsequent thermal or solvent annealing, or the incorporation of fractional amounts of additives to tune the nanoscale phase separation between and crystallization of the constituents.^{6,7,33} Solution deposition of the active layer in planar heterojunctions, on the other hand, is problematic as the solvent used during deposition of the top layer will necessarily erode the underlying layer. This issue can be addressed by designing chemically dissimilar electron donors and acceptors that enable the use of orthogonal solvents. A crosslinkable layer is another option for avoiding solvent damage during the deposition of subsequent layers.³⁴ As detailed below, ScL provides an alternative to the construction of planar-heterojunction devices as contact between organic layers are made in the absence of solvents. Finally, top electrodes are defined by evaporating metals through a shadow mask.

Soft-Contact Lamination

In ScL, an elastomeric support substrate, typically cross-linked polydimethylsiloxane, PDMS, is used as a carrier for a metal layer, an organic layer, or a multilayer structure. This elastomer can then be laminated against another substrate, making conformal contact. Held in place by van der Waals forces, no external pressure is required to establish contact. In this way, top metal electrodes can be reversibly contacted and removed from the underlying active layer, while solution processed organic multilayers that are otherwise inaccessible can be assembled by bringing together

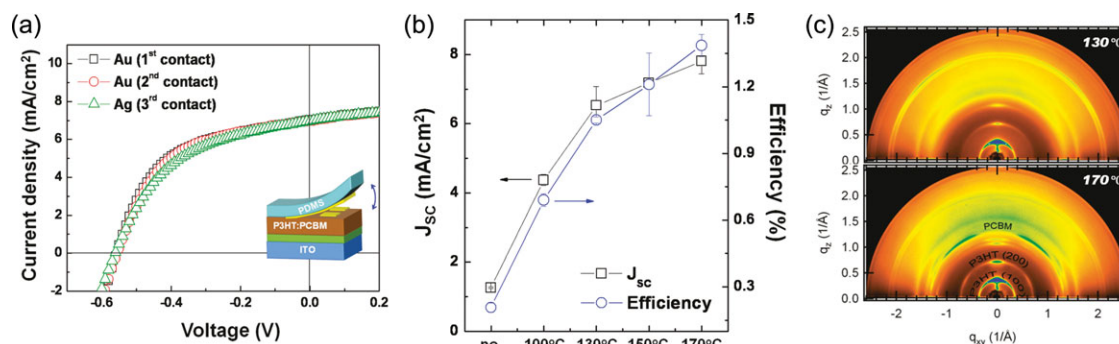


Figure 2. (a) J-V characteristics of a P3HT:PCBM inverted bulk-heterojunction solar cell after lamination of two separate gold electrodes and one silver electrode, all showing comparable device performance, (b) increase in J_{sc} (left axis) and efficiency (right axis) as annealing temperature is increased, and (c) GIXD patterns of once-buried P3HT:PCBM active layers after annealing in the presence of a top gold electrode at 130°C and 170°C.

Reprinted with permission from Ref. 39. Copyright 2010 American Chemical Society.

layers attached separately to an elastomer and a target substrate. The elastomer can then be peeled away, leaving the combination of organic layers on the new substrate. Through comparison of the molecular energy levels and electrical performance of organic semiconductor films processed by spin-coating and ScL, it has been established that ScL does not modify the electronic properties of the film.³⁵ In view of this, ScL has the potential to be a powerful tool for constructing and dissecting multilayer organic devices.

Electrode Lamination

Organic solar cell performance is highly sensitive to the active layer structure, which in turn depends on the processing details during device fabrication.^{6,7} In a completed device, however, the active layer is buried beneath the top electrode, and is inaccessible for direct characterization. The structure of the active layer is thus often inferred from the characterization of thin films that are subjected to conditions that closely approximate those used during the preparation of active layers in solar cells, albeit in the absence of a top electrode. Yet, the performance of organic solar cells that are thermally annealed before and after top electrode deposition is generally different,^{36–38} suggesting significant differences in active layer morphology resulting from dissimilar interfacial energy landscapes during annealing in the presence and absence of the top electrode. Non-invasive, direct characterization of the properties of buried films that were annealed in the presence of top contacts is thus essential for elucidating the fundamental structure-function relationships in functional organic solar cells. ScL enables the reversible attachment and removal of a top metal contact, making it possible to construct a working solar cell device, and then to subsequently remove the top electrode for structural investigation.

In order to study buried active layers, inverted BHJ solar cells were built using standard processing procedures. Instead of evaporating the top electrodes, however, gold or silver electrodes that were previously patterned on an elastomeric PDMS substrate were brought into contact with the active layer, as shown schematically in the inset of Figure 2a. The contact process is entirely reversible and robust,

meaning that the top metal electrode can be contacted to the active layer, removed, and recontacted with a different electrode to yield the same device performance, as seen in Figure 2a.³⁹

Thermal annealing of the device stack after electrode deposition has been shown to significantly increase the J_{sc} and efficiency of inverted solar cells (Figure 2b). Given prior inability to examine the buried active layers of such functional devices, this improvement in device characteristics has been speculated to stem from an increase in the crystallinity of the polymer donor. By peeling away the laminated electrodes, the once-buried active layer could be structurally characterized following device fabrication and testing. As observed in Figure 2c, grazing-incidence X-ray diffraction (GIXD) revealed strong P3HT (h00) reflections along the meridian, with an increased intensity at higher annealing temperatures, indicating that P3HT does indeed become more crystalline when subjected to thermal annealing and its crystallites become preferentially oriented with the molecular backbone edge-on with respect to the substrate. Diffuse PCBM reflections, seen in the once-buried active layers of devices annealed at 130°C, also sharpen significantly when annealing is carried out at 170°C, indicating its transition from being amorphous to an increasingly ordered structure. Azimuthal variations in intensity indicate preferential orientation of PCBM in the once-buried active layer. Although annealing is known to increase P3HT crystallinity, the substantial structural rearrangement of PCBM has not been observed before and is expected to relate to the presence of the top electrode during thermal annealing. Observation of such structural changes in the buried active layer that is enabled by ScL would not have been otherwise possible. The ScL approach to organic solar cell construction and deconstruction opens up a general route for accessing once-buried active layers and interfaces for structural characterization within functional devices.

As mentioned earlier, the sequence with which the active layers are annealed can have a significant effect on the performance of inverted P3HT:PCBM BHJ solar cells. In particular, the V_{oc} decreases substantially, from 0.55 V to 0.47 V when annealing at 130°C is performed after, rather than

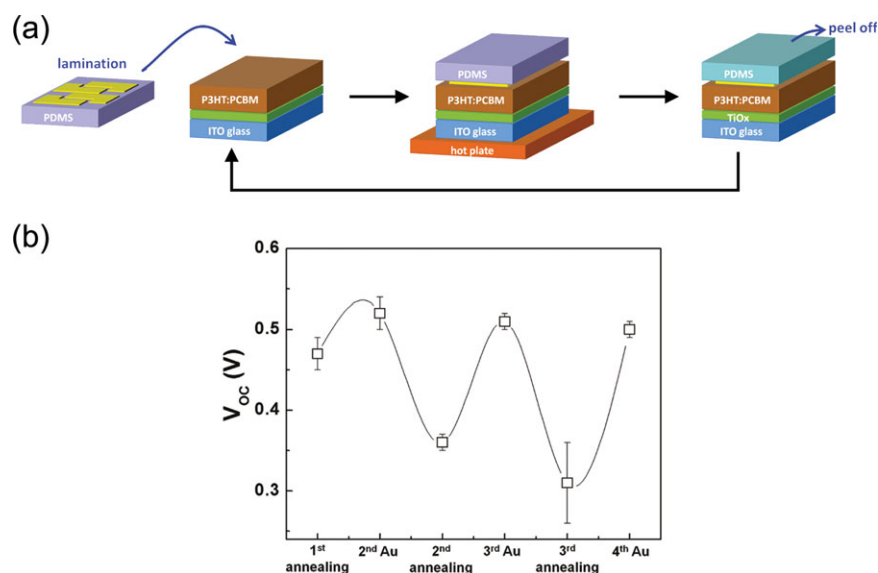


Figure 3. (a) Schematic of the cyclic process employed for top electrode lamination, device annealing, and top electrode replacement, and (b) Reversible decay and recovery of V_{oc} in a single inverted P3HT:PCBM solar cell after repeated annealing and fresh top electrode replacement.

Reprinted with permission from Ref. 36. Copyright 2011 American Chemical Society.

before, gold electrode deposition.³⁶ In principle, the V_{oc} is primarily dependent on the relative energy levels of the HOMO of the electron donor and LUMO of the electron acceptor. Nevertheless, such V_{oc} variations with device fabrication and processing conditions are commonly reported.^{37,38} Experiments for isolating the cause of such differences, however, have been lacking, largely because the interfaces in question are buried and inaccessible.

Taking advantage of the modularity and reversibility of ScL, sequences of top electrode lamination, device annealing, and top electrode delamination were repeated, with fresh top electrodes replacing old ones each time (see Figure 3). Surprisingly, when fresh contacts are incorporated into the device, its V_{oc} recovers to 0.52 V. Annealing in the presence of these contacts results in a drop in V_{oc} once again. This reversible decay and recovery of the V_{oc} on annealing and top electrode replacement, respectively, is shown in Figure 3b.³⁶

Given that the V_{oc} is restored when a fresh top contact is introduced, the origin for this decay cannot be in the bulk of the photoactive layer; the cause must be related to the active layer-top electrode interface. X-ray photoelectron spectroscopy (XPS) was carried out on once-buried device active layers and delaminated top electrodes to probe changes. Compared with unannealed once-buried P3HT:PCBM active layers, active layers annealed in the presence of gold electrodes exhibit a shift of the sulfur peaks toward higher binding energy, indicating that a chemical reaction has taken place between the thiophene units of the P3HT and gold upon annealing. Moreover, ultraviolet photoemission spectroscopy (UPS) measurements showed that annealing P3HT:PCBM active layers in the presence of gold electrodes increases the barrier for hole extraction while decreasing its work function. Taken together, these measurements show that annealing inverted solar cells following top gold electrode attachment leads to an interfacial

chemical reaction between P3HT and gold, resulting in a drop in the gold work function, and accordingly, a reduced device V_{oc} . Surprisingly, this adverse effect can be mitigated by replacement of the gold electrode after annealing.

Active Layer Lamination

In BHJ solar cells, phase separation drives the creation of nanoscale domains of electron donor and acceptor with a high density of donor-acceptor interfaces. Given that the active layers are typically only several hundred nanometers thick, surface energy can also affect structural development. Further complexities in the film structure may thus result in which the electron donor or acceptor preferentially segregates to the film surface or the film-substrate interface, driven by interfacial free energy differences.

Near-edge X-ray absorption fine structure spectroscopy (NEXAFS)⁴⁰ was used to quantify the relative surface coverage of P3HT and PCBM that arises from interfacial segregation in BHJ solar cell active layers.⁴¹ Consistent with prior reports,^{42–44} the prototypical P3HT:PCBM BHJ active layer consists of 97 wt % P3HT at the top surface. Using ScL, the active layer was delaminated and the once-buried bottom interface was exposed for further characterization. NEXAFS revealed that this interface consisted of 65 wt % P3HT. Thus, the top BHJ active layer surface is predominantly composed of P3HT, while the buried interface is slightly enriched in P3HT relative to the composition from which the film was cast, i.e., 55 wt % P3HT. Until recently, such enrichment in P3HT at the electron-collecting interface was thought to hinder electron collection, but with little direct experimental evidence to validate this hypothesis.

To assess the influence of interfacial segregation on BHJ device performance, devices were first constructed by

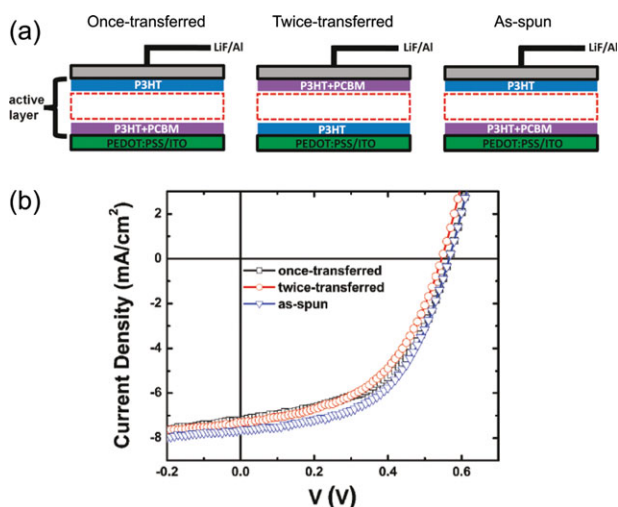


Figure 4. (a) Schematic illustrations of P3HT:PCBM bulk-heterojunction solar cells having once-transferred, twice-transferred, and as-spun active layers.

The once-transferred active layer is enriched in P3HT at the top surface, while the twice-transferred, i.e., flipped-over, active layer is enriched in P3HT at the bottom surface, and (b) solar cell characteristics in all three cases are comparable. Reprinted with permission from Ref. 41. Copyright 2011 American Chemical Society.

laminating NEXAFS-characterized active layers, having a strong enrichment in P3HT at the top surface, into devices, as shown in Figure 4. By performing two ScL transfer steps, the twice-transferred devices were constructed with the original active layer that had been flipped over. In this case, the P3HT-rich interface is now in direct contact with poly(ethylene dioxithiophene):poly(styrene sulfonic acid), PEDOT:PSS, the buffer layer intervening the active layer and ITO. For comparison, BHJ devices having the typical composition profile, obtained by directly spin-casting the active layer onto PEDOT:PSS/ITO, were considered as well.

In the once-transferred and as-spun devices, P3HT enhancement at the electron-collecting interface is expected to hinder electron flow given that P3HT transports holes more efficiently than electrons. Devices comprising the twice-transferred active layer should thus—in theory—be far superior since the hole-transporting P3HT-enriched layer is now in contact with the anode, where holes are collected. Solar cell characteristics, however, show little difference between the devices comprising spin-coated, once-, or twice-transferred active layers, as shown in Figure 4b. In other words, contrary to expectation, vertical phase separation does not affect P3HT:PCBM BHJ performance. In this case, ScL has uniquely enabled the comparison of performance of devices having active layers with reversed vertical phase separation characteristics.

Additional tests were conducted by laminating thin layers of organic semiconductor constituents at the electron- and hole-collecting interfaces. The addition of an 8–9 nm thick P3HT layer inserted at the electron-collecting interface results in J_{sc} decreases of less than 10%. Conversely, negative con-

trol experiments in which a 12–14 nm thick PCBM layer is inserted at the hole-collecting interface results in a severe drop in performance. These results imply an asymmetry in the charge transport capabilities of P3HT and PCBM, with P3HT allowing transport of electrons to the cathode while PCBM more effectively blocking hole transport to the anode.

Further study revealed that this asymmetry in charge transport likely stems from a broad distribution of electronic “tail states” that are present in P3HT but not in PCBM.⁴⁵ Given that P3HT is easily oxygen doped, such states carry holes that can recombine with electrons at the electron-collecting interface. Subsequent hole injection from the cathode replenishes the holes occupying the tail states and allows net current flow through the P3HT layer. In the prototypical P3HT:PCBM, this broad distribution of tail states in P3HT renders interfacial segregation nearly inconsequential to device operation. Solar cells comprising other organic semiconductors possessing broad electronic state distributions should thus exhibit similar invariant characteristics. ScL can be used as a tool to screen for this attribute by enabling the transfer of thin electron donor or acceptor layers to the electron-collecting or hole-collecting interfaces, or the reversal of active layer in cases where interfacial segregation is significant.

By using ScL to flip the P3HT:PCBM active layer, it has also been possible, for the first time, to directly measure the electronic structure of the blend. Because interfacial segregation leads to a strongly P3HT-enriched top surface, its electronic structure—often measured by spectroscopic techniques that are sensitive to the surface—is not necessarily representative of that of the blend interior. In fact, the HOMO and LUMO levels at the top surface of a P3HT:PCBM film were found to be comparable to those for a pure P3HT film.⁴⁶ Electronic characterization of the once-buried bottom surface of a P3HT:PCBM blend that was exposed by ScL, instead reveal HOMO energy level that is close to that of P3HT and a LUMO energy level near that of PCBM. The HOMO–LUMO energy gap is larger than what one would expect from comparing the energy levels of pristine P3HT and PCBM, however, indicating the formation of dipoles at the P3HT:PCBM interface. The finding that the electronic structure of the blend does not perfectly match the structure deduced from independent P3HT and PCBM films illustrates the importance of direct energy level determination of blends for accurate mapping of the energy landscape within solar cell active layers. In this case, the wider than expected energy gap implies a higher theoretical limit for the V_{oc} of P3HT:PCBM solar cells than previously thought based on energy levels extract from neat films of the constituent organic semiconductors.

An additional application of ScL is the assembly of planar-heterojunction solar cells. Such devices are normally not accessible through conventional solution processing, since the solubility of electron donors and acceptors in similar solvents precludes sequential deposition of multiple layers.⁴⁷ Using ScL, it is also possible to laminate together individual electron donor and acceptor layers whose thickness and processing conditions had been independently tuned. This approach affords a unique opportunity to study the influence of processing on the crystallinities of organic semiconductor constituents, and accordingly, organic solar cell performance

without structural complications arising from phase separation found in BHJ electron donor-acceptor active layers.

Planar-heterojunction solar cells were fabricated by transferring P3HT onto a PDMS substrate with prepatterned gold electrodes. The P3HT/Au-electrode/PDMS assembly was then laminated onto a PCBM/TiO_x/ITO/glass substrate to complete the planar-heterojunction solar cell.³⁹ In this particular system, P3HT films that are 160-nm thick were optimal, with thinner films not absorbing as much light, and thicker yet films presenting a high series resistance for carrier extraction. Polymer-polymer planar-heterojunction solar cells comprising P3HT and poly{[N,N'-bis(2-octyldodecyl)-naphthalene-1,4,5,8-bis(dicarboximide)-2,6-diyl]-*alt*-5,5'-[2,2'-bithiophene]}, P(NDI2OD-T2),⁴⁸ were also successfully constructed demonstrating the versatility of ScL for planar-heterojunction device fabrication.³⁹

ScL was used to study the effect of independent annealing of P3HT and PCBM layers on structure development in the respective layers and collective planar-heterojunction solar cell performance. Annealing was performed both in air and under nitrogen, although here we will focus only on the latter case, during which oxidation is not an issue. A significant finding was that planar-heterojunction devices with active layers comprised of annealed P3HT and unannealed PCBM showed little difference in J_{sc} from devices in which both layers were unannealed.⁴⁹ This observation was surprising given that annealing is expected to increase the crystallinity of P3HT, resulting in improved hole transport, and thus an increased J_{sc} . GIXD revealed that in the absence of PCBM, P3HT readily crystallizes upon spin-casting from chlorobenzene; subsequent annealing only modestly increases its crystallinity. As a result, J_{sc} is only weakly affected by annealing of the P3HT layer.

Analogous experiments were performed with devices comprised of unannealed P3HT and annealed PCBM layers. After 1 min of annealing, J_{sc} increased modestly, but then progressively decreased with further annealing of the PCBM layer. GIXD corroborated that PCBM evolves from amorphous, to a structure featuring nanoscale crystallites after thermal annealing for 1 min; and preferentially oriented crystals that result upon further annealing.

Surprisingly, the presence of preferentially oriented PCBM crystals in the active layer is associated with the lowest J_{sc} in solar cell performance. Although a highly-ordered molecular arrangement is normally expected to improve charge transport, in this case the opposite trend was observed, demonstrating the importance of not just constituent crystallinity, but also molecule and crystal orientation. Electron mobilities extracted from PCBM single-carrier diodes directly mirrored the J_{sc} trend in planar-heterojunction solar cells, further confirming reduced out-of-plane transport associated with the presence of such oriented PCBM crystallites.

Outlook

ScL is a valuable tool for constructing and deconstructing organic solar cells for gleaning fundamental insight into structure-function relationships, providing access to formerly-buried active layers, as well as device configurations

that are otherwise not possible. Further directions of study include the systematic lamination and delamination of different electrode materials, including chemically-modified top electrodes. Additional work on buried interfaces will aid the design and improvement of buffer layers, enable the assessment of interfacial segregation effects in new materials systems, and allow further systematic study of planar-heterojunction solar cells where structural effects can be assessed without the complications that arise from electron donor-acceptor phase separation.

Beyond these fundamental benefits, ScL also opens up new technological avenues, such as the fabrication of novel tandem organic solar cells and the integration of new materials. Improved optical absorption and solar cell efficiency can be achieved by using a tandem solar cell architecture whereby two stacked solar cells, with responses to complementary regions of the solar spectrum, are integrated together.⁹ To-date, tandem BHJ organic solar cells have yielded the highest efficiencies. On the other hand, tandem organic solar cells are exceedingly difficult to construct as they rely on a many-layered structure whose processing is far more complex compared to that of single-cell architecture. This challenge is exacerbated by the problem of preparing multilayered architectures from solution without the solvents affecting previously-cast layers. ScL may offer the possibility of assembling the separate halves of the tandem cell on separate substrates and then laminating them together. Alternatively, layers may be built up in a sequential fashion by organic layer transfer.

One can also consider incorporating new materials into organic solar cells via ScL. Alternatives to ITO are widely being sought as a transparent electrode material, given the relative scarcity of indium and the brittleness of the transparent metal oxide. Graphene, for example, is considered a strong candidate whose incorporation will also allow the fabrication of mechanically flexible devices.⁵⁰ High-quality, large-area graphene can be produced by chemical-vapor deposition onto particular metal substrates, such as copper and ruthenium.^{51,52} Subsequent integration into devices requires the transfer of graphene onto another substrate, either by carrying it on a sacrificial support, or via lamination.^{53,54} A roll-to-roll transfer process, relying on a thermal release tape support, has already been demonstrated, enabling graphene integration into a fully functional large-area touchscreen panel.⁵⁵ Exciting prospects exist for extending such roll-to-roll processes to laminating graphene and organic semiconductor layers for the low cost, high-throughput fabrication of large-area organic solar cells.

Acknowledgments

We acknowledge support from the Photovoltaics Program at the ONR (N00014-11-10328), and the SOLAR Initiative at the NSF (DMR-1035217). J.M.M. is supported by the Camille and Henry Dreyfus Postdoctoral Program in Environmental Chemistry.

Literature Cited

1. Forrest SR. The path to ubiquitous and low-cost organic electronic appliances on plastic. *Nature*. 2004; 428:911.

2. Krebs FC, Tromholt T, Jorgensen M. Upscaling of polymer solar cell fabrication using full roll-to-roll processing. *Nanoscale*. 2010;2:873.
3. Krebs FC. Fabrication and processing of polymer solar cells: A review of printing and coating techniques. *Solar Energy Mater Sol Cells*. 2009;93:394.
4. Scharber MC, Wuhlbacher D, Koppe M, Denk P, Waldauf C, Heeger AJ, Brabec CL. Design rules for donors in bulk-heterojunction solar cells - Towards 10% energy-conversion efficiency. *Adv Mater*. 2006;18:789.
5. Boudreault PLT, Najari A, Leclerc M. Processable low-bandgap polymers for photovoltaic applications. *Chem Mater*. 2011;23:456.
6. Hoppe H, Sariciftci NS. Morphology of polymer/fullerene bulk heterojunction solar cells. *J Mater Chem*. 2006;16:45.
7. Yang X, Loos J. Toward high-performance polymer solar cells: The importance of morphology control. *Macromolecules*. 2007;40:1353.
8. Yu G, Gao J, Hummelen JC, Wudl F, Heeger AJ. Polymer photovoltaic cells - Enhanced efficiencies via a network of internal donor-acceptor heterojunctions. *Science*. 1995;270:1789.
9. Kim JY, Lee K, Coates NE, Moses D, Nguyen TQ, Dante M, Heeger AJ. Efficient tandem polymer solar cells fabricated by all-solution processing. *Science*. 2007;317:222.
10. Bourzac K. A leap forward for plastic solar cells. *Technol Rev*. 2012; <http://www.technologyreview.com/news/427032/a-leap-forward-for-plastic-solar-cells/>.
11. Brabec CJ, Hauch JA, Schilinsky P, Waldauf C. Production aspects of organic photovoltaics and their impact on the commercialization of devices. *MRS Bulletin*. 2005;30:50.
12. Loo Y-L, Someya T, Baldwin KW, Bao ZN, Ho P, Dodabalapur A, Katz HE, Rogers JA. Soft, conformable electrical contacts for organic semiconductors: High-resolution plastic circuits by lamination. *Proc Nat Acad Sci USA*. 2002;99:10252.
13. Zaumseil J, Someya T, Bao ZN, Loo Y-L, Cirelli R, Rogers JA. Nanoscale organic transistors that use source/drain electrodes supported by high resolution rubber stamps. *Appl Phys Lett*. 2003;82:793.
14. Zaumseil J, Baldwin KW, Rogers JA. Contact resistance in organic transistors that use source and drain electrodes formed by soft contact lamination. *J Appl Phys*. 2003;93:6117.
15. Guo TF, Pyo S, Chang SC, Yang Y. High performance polymer light-emitting diodes fabricated by a low temperature lamination process. *Adv Funct Mater*. 2001;11:339.
16. Lee TW, Zaumseil J, Bao ZN, Hsu JWP, Rogers JA. Organic light-emitting diodes formed by soft contact lamination. *Proc Nat Acad Sci USA*. 2004;101:429.
17. Kim J, Khang DY, Kim JH, Lee HH. The surface engineering of top electrode in inverted polymer bulk-heterojunction solar cells. *Appl Phys Lett*. 2008;92:133307.
18. Huang JS, Li G, Yang Y. A semi-transparent plastic solar cell fabricated by a lamination process. *Adv Mater*. 2008;20:415.
19. Gelinck G, Heremans P, Nomoto K, Anthopoulos TD. Organic transistors in optical displays and microelectronic applications. *Adv Mater*. 2010;22:3778.
20. Dodabalapur A. Negatively successful. *Nature*. 2005;434:151.
21. Walker B, Kim C, Nguyen TQ. Small molecule solution-processed bulk heterojunction solar cells. *Chem Mater*. 2011;23:470.
22. Brabec CJ, Gowrisanker S, Halls JJM, Laird D, Jia SJ, Williams SP. Polymer-fullerene bulk-heterojunction solar cells. *Adv Mater*. 2010;22:3839.
23. Lunt RR, Giebink NC, Belak AA, Benziger JB, Forrest SR. Exciton diffusion lengths of organic semiconductor thin films measured by spectrally resolved photoluminescence quenching. *J Appl Phys*. 2009;105:053711.
24. Scully SR, McGehee MD. Effects of optical interference and energy transfer on exciton diffusion length measurements in organic semiconductors. *J Appl Phys*. 2006;100:034907.
25. Po R, Carbonera C, Bernardi A, Camaioni N. The role of buffer layers in polymer solar cells. *Energy Environ Sci*. 2011;4:285.
26. Lee SS, Loo Y-L. Structural complexities in the active layers of organic electronics. *Annu Rev Chem Biomol Eng*. 2010;1:59.
27. Brabec CJ, Cravino A, Meissner D, Sariciftci NS, Fromherz T, Rispen MT, Sanchez L, Hummelen JC. Origin of the open circuit voltage of plastic solar cells. *Adv Funct Mater*. 2001;11:374.
28. Gadisa A, Svensson M, Andersson MR, Inganäs O. Correlation between oxidation potential and open-circuit voltage of composite solar cells based on blends of polythiophenes/fullerene derivative. *Appl Phys Lett*. 2004;84:1609.
29. Ramsdale CM, Barker JA, Arias AC, MacKenzie JD, Friend RH, Greenham NC. The origin of the open-circuit voltage in polyfluorene-based photovoltaic devices. *J Appl Phys*. 2002;92:4266.
30. Jorgensen M, Norrman K, Krebs FC. Stability/degradation of polymer solar cells. *Sol Energy Mater Solar Cells*. 2008;92:686.
31. Kim CS, Lee SS, Gomez ED, Kim JB, Loo Y-L. Transient photovoltaic behavior of air-stable, inverted organic solar cells with solution-processed electron transport layer. *Appl Phys Lett*. 2009;94:113302.
32. Hau SK, Yip HL, Baek NS, Zou JY, O'Malley K, Jen AKY. Air-stable inverted flexible polymer solar cells using zinc oxide nanoparticles as an electron selective layer. *Appl Phys Lett*. 2008;92:253301.
33. Peet J, Kim JY, Coates NE, Ma WL, Moses D, Heeger AJ, Bazan GC. Efficiency enhancement in low-bandgap polymer solar cells by processing with alkane dithiols. *Nat Mater*. 2007;6:497.
34. Kim BJ, Miyamoto Y, Ma BW, Frechet MJM. Photocrosslinkable polythiophenes for efficient, thermally stable, organic photovoltaics. *Adv Funct Mater*. 2009;19:2273.
35. Shu A, Dai A, Wang H, Loo Y-L, Kahn A. Electronic structure and carrier transport at laminated polymer homojunctions. *Org Electron*. Accepted 2012.
36. Kim JB, Guan ZL, Shu AL, Kahn A, Loo Y-L. Annealing sequence dependent open-circuit voltage of inverted polymer solar cells attributable to interfacial chemical reaction between top electrodes and photoactive layers. *Langmuir*. 2011;27:11265.

37. McNeill CR, Halls JJM, Wilson R, Whiting GL, Berkebile S, Ramsey MG, Friend RH, Greenham NC. Efficient polythiophene/polyfluorene copolymer bulk heterojunction photovoltaic devices: Device physics and annealing effects. *Adv Funct Mater.* 2008;18:2309.
38. Orimo A, Masuda K, Honda S, Benten H, Ito S, Ohkita H, Tsuji H. Surface segregation at the aluminum interface of poly(3-hexylthiophene)/fullerene solar cells. *Appl Phys Lett.* 2010;96:043305.
39. Kim JB, Lee S, Toney MF, Chen ZH, Facchetti A, Kim YS, Loo Y-L. Reversible soft-contact lamination and delamination for non-invasive fabrication and characterization of bulk-heterojunction and bilayer organic solar cells. *Chem Mater.* 2010;22:4931.
40. Loo Y-L. Structural elucidation of active layers in organic electronic devices via NEXAFS. IOP Conf. Series. *Mater Sci Eng.* 2010;14:012018.
41. Wang H, Gomez ED, Kim J, Guan ZL, Jaye C, Fischer DA, Kahn A, Loo Y-L. Device characteristics of bulk-heterojunction polymer solar cells are independent of interfacial segregation of active layers. *Chem Mater.* 2011;23:2020.
42. Campoy-Quiles M, Ferenczi T, Agostinelli T, Etchegoin PG, Kim Y, Anthopoulos TD, Stavrinou PN, Bradley DDC, Nelson J. Morphology evolution via self-organization and lateral and vertical diffusion in polymer: fullerene solar cell blends. *Nat Mater.* 2008;7:158.
43. Germack DS, Chan CK, Hamadani BH, Richter LJ, Fischer DA, Gundlach DJ, DeLongchamp DM. Substrate-dependent interface composition and charge transport in films for organic photovoltaics. *Appl Phys Lett.* 2009;94:233303.
44. Xu Z, Chen LM, Yang GW, Huang CH, Hou JH, Wu Y, Li G, Hsu CS, Yang Y. Vertical phase separation in poly(3-hexylthiophene): Fullerene derivative blends and its advantage for inverted structure solar cells. *Adv Funct Mater.* 2009;19:1227.
45. Wang H, Shah M, Ganesan V, Chabinyc M, Loo Y-L. Tail state-assisted charge injection and recombination at the electron-collecting interface of P3HT:PCBM bulk-heterojunction polymer solar cells. *Adv Eng Mater.* 2012;doi:10.1002/aenm.201200361.
46. Guan ZL, Kim JB, Wang H, Jaye C, Fischer DA, Loo YL, Kahn A. Direct determination of the electronic structure of the poly(3-hexylthiophene):phenyl-[6,6]-C61 butyric acid methyl ester blend. *Org Electron.* 2010;11:1779.
47. Lee KH, Schwenn PE, Smith ARG, Cavaye H, Shaw PE, James M, Krueger KB, Gentle IR, Meredith P, Burn PL. Morphology of all-solution-processed "bilayer" organic solar cells. *Adv Mater.* 2011;23:766.
48. Yan H, Chen ZH, Zheng Y, Newman C, Quinn JR, Dotz F, Kastler M, Facchetti A. A high-mobility electron-transporting polymer for printed transistors. *Nature.* 2009;457:679.
49. Kim JB, Guan ZL, Lee S, Pavlopoulou E, Toney MF, Kahn A, Loo Y-L. Modular construction of P3HT/PCBM planar-heterojunction solar cells by lamination allows elucidation of processing-structure-function relationships. *Org Electron.* 2011;12:1963.
50. Pang SP, Hernandez Y, Feng XL, Mullen K, Graphene as transparent electrode material for organic electronics. *Adv Mater.* 2011;23:2779.
51. Li XS, Cai WW, An JH, Kim S, Nah J, Yang DX, Piner R, Velamakanni A, Jung I, Tutuc E, Banerjee SK, Colombo L, Ruoff RS. Large-area synthesis of high-quality and uniform graphene films on copper foils. *Science.* 2009;324:1312.
52. Sutter PW, Flege JI, Sutter EA. Epitaxial graphene on ruthenium. *Nat Mater.* 2008;7:406.
53. Reina A, Jia XT, Ho J, Nezich D, Son HB, Bulovic V, Dresselhaus MS, Kong J. Large area, few-layer graphene films on arbitrary substrates by chemical vapor deposition. *Nano Lett.* 2009;9:30.
54. Kim KS, Zhao Y, Jang H, Lee SY, Kim JM, Kim KS, Ahn JH, Kim P, Choi JY, Hong BH. Large-scale pattern growth of graphene films for stretchable transparent electrodes. *Nature.* 2009;457:706.
55. Bae S, Kim H, Lee Y, Xu XF, Park JS, Zheng Y, Balakrishnan J, Lei T, Kim HR, Song YI, Kim YJ, Kim KS, Ozyilmaz B, Ahn JH, Hong BH, Iijima S. Roll-to-roll production of 30-inch graphene films for transparent electrodes. *Nat Nanotechnol.* 2010;5:574.

